

Deviations from Hubble Flow in the Local Universe

Riccardo Giovanelli
Cornell University

October 11, 2018

1 Introduction

Beginning with the pioneering efforts of Rubin *et al.* (1976), the study of large-scale deviations from Hubble flow has achieved undeniable observational successes (see reviews by Dekel 1994, Strauss and Willick 1995). In the spirit of providing fertile ground for discussion and further developments, this presentation will concentrate on few of the areas where a measure of variance of opinion exists, rather than on presenting a survey of results.

The determination of the peculiar velocity of galaxies over volumes of cosmological interest is an exercise fraught with large amplitude uncertainties. These arise from errors in the measurements, poorly understood corrections applied to the observed parameters, “cosmic” sources related to the formation history of each galaxy and to its individual peculiarities, and statistical corrections related to the variations in the galaxy density field. The most commonly applied methods, which use the Tully–Fisher (1977;TF) relation for spirals and the D_n – σ (Dressler *et al.* 1987) or the Fundamental Plane (FP; Djorgovski and Davis 1987) relations for spheroidals, lack a well developed physical basis, and an understanding of the impact of individual sources of scatter has been hazy at best. It is of paramount importance that the characteristics of the error budget of peculiar velocity measurement techniques be well understood, in order both to correctly infer the predictive power of the method and to derive reliable statistical corrections. In section 2, the error budget of the TF relation will be analyzed in detail.

The TF technique for spirals or the FP method for spheroidals requires a calibrated *template relation*. Offsets with respect to it are converted to peculiar velocities by means of exponential laws. It is well known that the estimate of peculiar velocities is independent on the assumed value of the

Hubble constant H_0 , but it needs a kinematical calibration in order for the *velocity zero point* to be established. This requires that a set of objects be found, that can be globally assumed to yield a TF zero-point offset, consistent with rest in the comoving reference frame. This is a toilful task, the limits of which will be tackled in section 3.

Occasionally, warning signals go off indicating that not all is well with the standard expectations of predictive power of peculiar velocity measurement techniques. For example, the peculiar velocity of a system as measured by using its population of spiral galaxies may differ from that obtained using its population of spheroidals, the discrepancy being well in excess of the statistical errors associated with each technique. It is thus legitimate to ask: are we comfortable that spirals and spheroidals in general yield the same “observed” peculiar velocity field? We consider this question in section 4.

The distribution function of the cluster peculiar velocities, which are measured with significantly better accuracy than those of individual galaxies, has been used as a discriminant between different cosmological models. In section 5, we review recent results on cluster velocities that provide relatively tight constraints on models.

The early suggestion of Scaramella *et al.* (1989), that local motions may maintain coherence over scales in excess of $10,000 \text{ km s}^{-1}$, have received corroborating support from several sources, most notably Lauer and Postman (1994). In section 6 we review the evidence for large scale bulk flows and the issue of convergence depth in the local universe, as indicated by all-sky samples of relatively nearby spirals ($cz \leq 9,000 \text{ km s}^{-1}$), both in and outside clusters.

The last few years have seen the unfolding of a massive effort in the measurement of primary galaxy distances, with the principal aim of reducing the uncertainty on the value of the Hubble constant. This has also allowed a significantly improved absolute calibration of the zero point of the TF relation, i.e. of the ability of using the relation to measure *distances*, rather than just peculiar velocities. The availability of an increasingly accurate TF template relation and peculiar velocity estimates to clusters such as Virgo and Fornax allow us to test the linearity of the Hubble flow over distances several times larger than those sampled by primary indicators and more accurate TF estimates of the value of H_0 . We indulge in this exercise in section 7.

Finally, in Section 8 we briefly report on ongoing efforts to improve the definition of the local peculiar velocity field, as well as to establish a TF template based on a set of clusters at $cz > 10,000 \text{ km s}^{-1}$, which will

provide a reference frame of the increased quality for all TF work.

2 The Error Budget of the TF Relation

An assessment of the predictive power of the TF method and an adequate estimate of its biases require a fair understanding of the nature of its associated scatter. That scatter arises from several sources: errors in the measurements of the TF parameters and uncertainties associated with the corrections applied to them combine with variance in the galactic properties produced by differences in the formation and evolution processes. The latter is often referred to as the *intrinsic* contribution to scatter; while it can in principle be reduced by flagging objects with observable anomalies such as velocity field distortions, deviations from disk planarity, other gravitational and photometric asymmetries, etc., this approach is seldom carried out to extensive lengths, especially when large samples of objects are studied. Several misconceptions regarding the nature of the TF scatter appear in the literature: that it is well represented by a single number; that the measurement and correction errors fully account for the observed dispersion; that only errors on the velocity widths are important. Giovanelli *et al.* (1996a; see also Rhee 1996) have made a detailed appraisal of the sources of I band TF scatter. They find that: (i) the total TF scatter cannot be represented by a single value; rather, it varies monotonically with velocity width, varying by a factor of 2 between ends of the range of widths typically used in TF applications; the average value of the r.m.s. scatter is in the neighborhood of 0.35 mag, while its value for the galaxies of higher velocity width approaches 0.25 mag; (ii) measurement and processing errors are important contributors, but they do not fully account for the amplitude of the scatter; (iii) uncertainties on magnitude can be important drivers of the total scatter, especially for luminous, highly inclined galaxies; (iv) the case for an inverse TF relation that may be assumed to be bias-free is weakened by the characteristics of the TF scatter. These results have an important impact in the calculation of bias corrections, particularly on the Malmquist bias correction for objects in the far sides of sampled volumes, as well as in applications of the TF method for the estimate of H_0 (Giovanelli 1996 and [11]).

3 A TF Template Relation

The construction of a template relation is the most delicate aspect of a TF program. It requires careful treatment of the effect of bias, which demands an adequate understanding of the sources of scatter, and a kinematically satisfactory reference frame. While template calibrations that use field galaxies have been used in the past, procedures that yield a template from cluster galaxy samples are generally preferred. The latter approach requires that: (a) the cluster environment does not alter the TF behavior of member galaxies, so that the derived template can also be applied to field objects; (b) bias corrections be separately estimated for each cluster; (c) cluster motions with respect to the comoving reference frame be measured and accounted for, before each cluster's galaxies are incorporated in the definition of the template. A template TF relation, shown in Figure 1 and based on a sample of 555 galaxies in 24 clusters, with cz between 1,000 and 10,000 km s⁻¹, was produced by [11]. They also verified that no environmental effects produce detectable differences among different clusters or between inner and outer regions of clusters.

A flawed template can severely distort the observed V_{pec} field. Errors in the TF slope or offset will produce spurious V_{pec} , of amplitude which will be generally variable with the target galaxy's velocity width. In all-sky samples, such spurious velocities can be spotted because of their characteristic geocentric signatures. In samples that are restricted in their sky coverage, on the other hand, spurious modulations of the velocity field are more difficult to identify, and they can easily be (and in some cases have been) confused with bulk flows. The combined uncertainty on TF slope and zero point offset, the latter constrained by sample size as well as by uncertainties in the cluster bias corrections and the quality of the kinematical calibration of the cluster set, is of ~ 0.07 mag; this converts to an uncertainty on V_{pec} of $\sim 3\%$ of cz .

One of the principal contributors to the above mentioned uncertainty is that associated with the kinematical calibration. When a single cluster is used as a reference (Coma is a frequent choice in that case), the inferred velocity field is tied to a kinematical reference frame where that cluster is at rest. Now, an object of radial velocity cz and peculiar velocity V_{pec} will yield a TF magnitude offset from the perfect template: $\delta m = 5 \log(1 + V_{pec}/cz)$, so that $|\delta m|$ will decrease with increasing cz . If the reference cluster V_{pec} is a priori unknown, the resulting template will predict velocities with an associated systematic uncertainty which, when expressed in magnitudes,

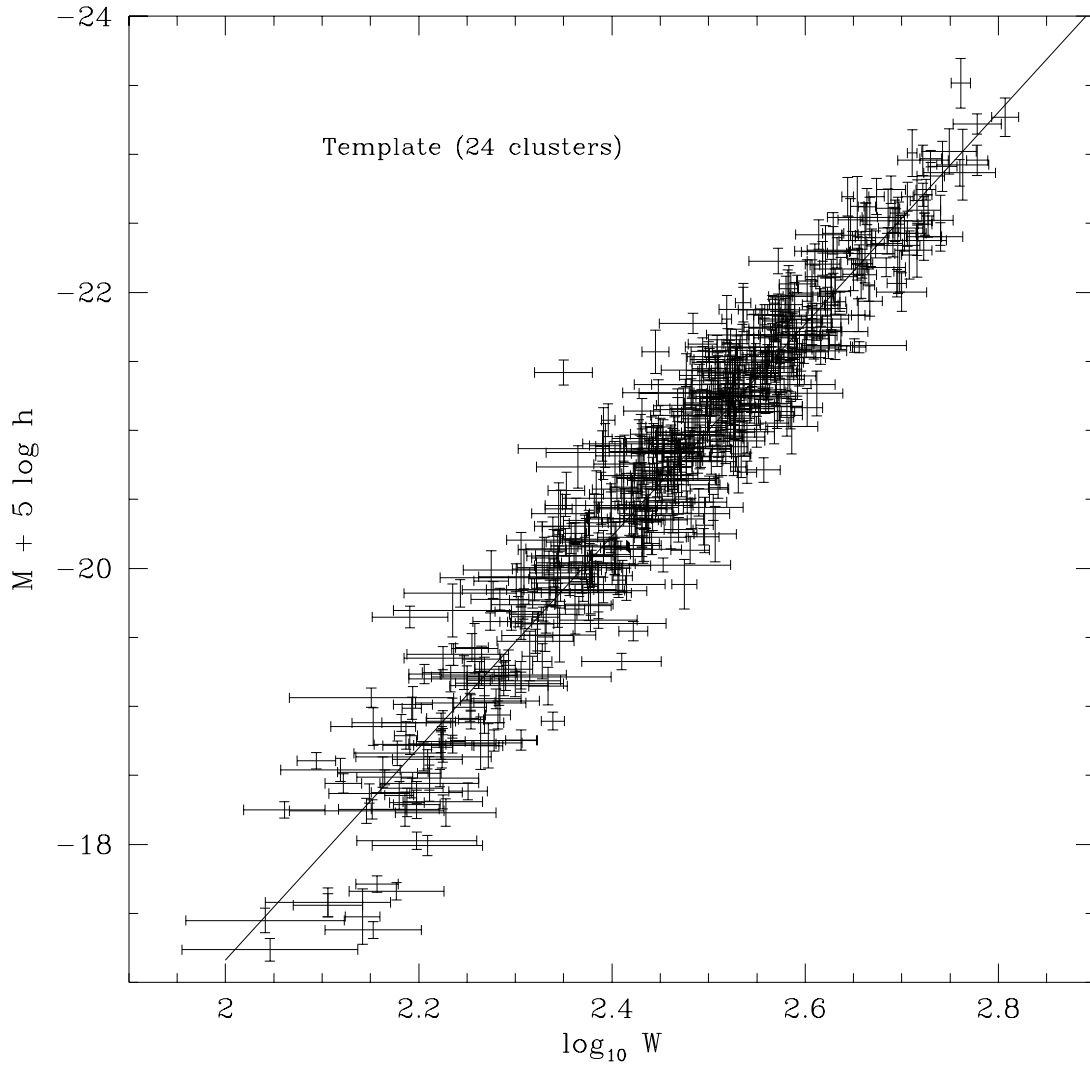


Figure 1: Template relation based on 555 galaxies in 24 clusters (after [11]).

will be reduced if the reference cluster is located at higher redshift. Ideally, the kinematical reference frame would thus be obtained using many *distant* clusters spread evenly over the sky, so that the uncertainty on the average δm would approach zero. Let N randomly distributed clusters be characterized by a 1-d peculiar velocity distribution function of r.m.s. $< V_{pec}^2 >^{1/2}$ km s⁻¹; to the first order, their a priori unknown motions will introduce a template zero point uncertainty of ([11])

$$\Delta m \sim 2.17 < V_{pec}^2 >^{1/2} < cz >^{-1} N^{-1/2} \text{ mag}, \quad (1)$$

where $< cz >$ is the average cluster redshift. In [11], a subset of 14 clusters located between 4,000 and 10,000 km s⁻¹ was used to establish the kinematical reference. Allowing for a measure of correlation in the cluster distribution, estimates of Δm vary between 0.03 and 0.06 mag. It is desirable, as we will discuss in section 8, to extend the sample to include clusters beyond 10,000 km s⁻¹.

4 Do Spirals and Ellipticals Yield the Same V_{pec} Field?

Peculiar velocities of galaxies have been extensively measured using two techniques: TF for spirals and FP (or D_n - σ) for spheroidals. Spiral and spheroidal samples are often combined to obtain denser coverage of the V_{pec} field. However, unsettling indications that the two techniques may not yield agreeable results to within the expected level of accuracy have appeared in the literature. In Figure 2, we plot data, adapted from Mould *et al.* (1991), which shows values of V_{pec} estimated using separately spiral and spheroidal samples, for a number of clusters; to the clusters in [20], we have added the notorious case of A2634, studied by Lucey *et al.* (1991). The unflattering nature of the comparison, first pointed out by Mould *et al.*, suggests several possibilities, including some worrisome ones, e.g. that the assumption of universality for the techniques that measure V_{pec} is invalid or that the impact of systematic errors may have been grossly underestimated.

Marco Scodeggio has applied his Ph.D. dissertation effort at Cornell to the investigation of this important issue. For each of six clusters with large, extant TF data sets, he has obtained independent FP galaxy distances, carrying out a detailed comparison of the spiral and spheroidal distances. In the particularly deviant case of A2634, a deep redshift survey was carried out (Scodeggio *et al.* 1995) in order to accurately characterize the structure

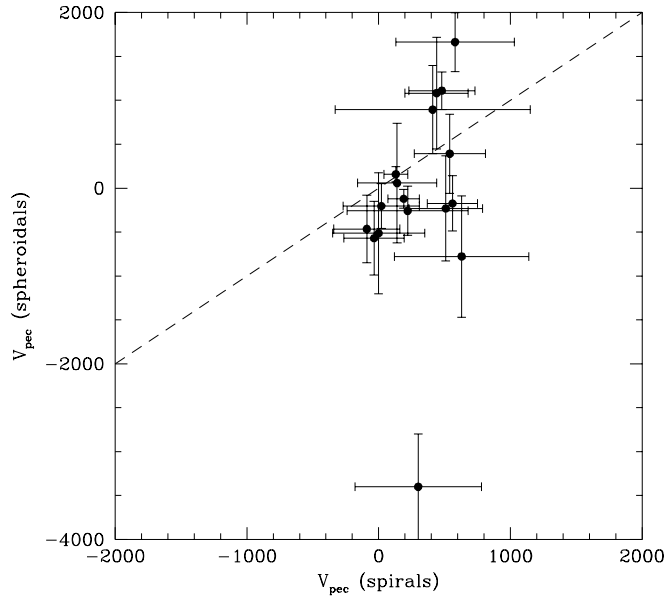


Figure 2: Comparison of V_{pec} measurements for clusters, using spiral and spheroidal samples. The figure is adapted after Table 7 and fig. 6 of [20], with the addition of the cluster A2634, the lowest point in the graph, with the velocity from spheroids of [17] and the velocity from spirals of [1].

of the cluster. It was then possible to rule out that the spiral and the spheroidal populations belong to separate dynamical entities, as well as to make accurate membership assignments. In A2634, new spheroidal velocity dispersions were obtained for 55 galaxies and the TF sample of [11] was extended to include 28 cluster spirals. Scodeggio *et al.* (1996) were able to verify that the new spheroidal and spiral samples yielded compatible values of V_{pec} . The comparison was corroborated in the case of the Coma cluster, for which 109 spheroidal and 41 spiral distances were available. It was also verified by [26] and [13] that there is no significant dependence of the FP parameters on cluster environment. These results place much of the blame of the problem illustrated in fig. 2 on the data quality of early spheroidal samples. For more recent, higher quality V_{pec} data, spiral and spheroidal galaxies appear now to yield compatible results.

5 The Cluster Velocity Distribution Function

The integrated, peculiar velocity distribution function of clusters of galaxies $P(> v)$ yields the relative number density of clusters with 3-dimensional $V_{pec} > v$. This quantity can be estimated for a variety of cosmological models. The observed distribution function refers to the 1-dimensional, radial velocity component, which we here refer to as $P(> v_{1d})$. Bahcall *et al.* (1994) and Moscardini *et al.* (1996) have recently produced estimates of the expected $P(> v)$ for a variety of cosmological models. Fig. 1b of Bahcall and Oh (1996) displays the function $P(> v_{1d})$, computed from the data of [11]. It can be noted that:

- (i) There are no clusters with peculiar velocity larger than about 600 km s⁻¹. Given the size of our sample, one can set a conservative limit of $P(> v_{1d}) \leq 0.05$ for $v_{1d} > 600$ km s⁻¹. This is in contrast with the values of V_{pec} shown in fig. 3, for example.
- (ii) Comparison of the observed $P(> v_{1d})$ with theoretical distribution functions computed for various cosmological models is inconsistent with high Ω_0 models. Similar results are obtained by [19], who also find the same data consistent only with models with $\Omega_0 \leq 0.4$.
- (iii) The observed 1-dimensional r.m.s. peculiar velocity of clusters is, according to [3], $\langle v_{1d}^2 \rangle^{1/2} = 293 \pm 28$ km s⁻¹.
- (iv) Previous measurements of cluster $P(> v_{1d})$ yielded a broader distribution, with a high velocity tail. The higher accuracy of the measurements reported here suggests that the high velocity tail was a spurious feature.

(v) The cluster $P(> v_{1d})$ suggested by the density reconstruction of Branchini *et al.* (1996, reported in [19]), has a high velocity tail, which is in disagreement with our cluster data. A velocity distribution with a high velocity tail, allowing for significant power $P(> v_{1d}) \geq 0.1$ at $v_{1d} \sim 1000 \text{ km s}^{-1}$, would appear to be necessary for consistency with high Ω_o models.

Our cluster $P(> v_{1d})$, which suggests low Ω_o models, is consistent with other cosmological cluster constraints; the discrepancy between the high baryon content of clusters of galaxies and the low baryon density required by primordial nucleosynthesis of light elements, for example, appears to be understandable only if either the universe has low density or if the standard interpretation of primordial nucleosynthesis is incorrect ([30],[16]). It is however in disagreement with previous measurements of cluster $P(> v_{1d})$ and with derivations of the value of Ω_o from global mapping of the peculiar velocity field and density field reconstructions obtained by using, for example, the Potent approach ([7]). These discrepancies are not yet well understood, and suggest that the reliability of the measured and inferred characteristics of the large-scale peculiar velocity field still need to be considered with a measure of caution.

6 Convergence Depth

6.1 Background

If the number density of galaxies $\delta_N(\mathbf{r})$ is known, and if it can be assumed that light traces mass via a constant bias parameter b , the peculiar velocity induced on the Local Group by the distribution of masses out to distance R can be written as

$$\mathbf{V}_{pec,LG}(R) = \frac{H_o \Omega_o^{0.6}}{4\pi b} \int \delta_N(\mathbf{r}) \frac{\hat{\mathbf{r}}}{r^2} W(r, R) d\mathbf{r}, \quad (2)$$

where $W(r, R)$ is a window function, e.g. $W(r, R) = \exp(-r^2/2R^2)$, and $\hat{\mathbf{r}}$ is the unit vector. The asymptotic value of $\mathbf{V}_{pec,LG}(R)$, for $R \rightarrow \infty$ can then be matched to the velocity inferred from the CMB dipole moment and an estimate of $\beta = \Omega_o^{0.6}/b$ can be obtained. Note that the gravitational effect of a galaxy is $\propto M_{gal}r^{-2}$; if $M_{gal} \propto L_{gal}$, then the gravitational contribution of that galaxy to $\mathbf{V}_{pec,LG}$ is proportional to its flux. In principle, $\mathbf{V}_{pec,LG}(\infty)$ can be gauged from a catalog of positions and fluxes of galaxies, or any other widely distributed extragalactic population, such as clusters. Given the discrete character of those distributions, in practical terms eqn. (2) is replaced

by a summation over the sampled objects, which is usually expressed in terms of the monopole $\mathcal{M}(R)$ and the dipole $\mathcal{D}(R)$ of the distribution:

$$V_{pec,LG}(R) = (1/3) \beta H_0 R \frac{\mathcal{D}(R)}{\mathcal{M}(R)}, \quad (3)$$

where

$$\mathcal{D}(R)/\mathcal{M}(R) = \left(3 \sum \frac{w_i \hat{r}_i}{r_i^2}\right) \left(\sum \frac{w_i}{r_i^2}\right)^{-1}, \quad (4)$$

the summations apply over all sampled objects within the distance R and w_i is a suitable weight, which may account for the selection function of the catalog and the luminosity of the object. With increasing R , the monopole term tends to $4\pi\bar{N}R$, where \bar{N} is the average number density of objects.

Calculations of $V_{pec,LG}(R)$ as described above have been carried out using different catalogs, yielding diverse results. When the predicted $V_{pec,LG}(\infty)$ are matched to the CMB dipole, clusters of galaxies require a scaling by $\beta_c \simeq 0.3$ (Tini Brunozzi et al. 1995), optically selected galaxies are better fitted by $\beta_{opt} \simeq 0.5$ (Scaramella *et al.* 1994) and IRAS selected galaxies agree with even higher values of $\beta_{ir} \sim 0.9$, suggesting varying degrees of bias between those populations and the mass distribution (see also discussion in Strauss, this volume). As for the distance to which eqns. (2) and (3) need to be integrated for the LG peculiar velocity to approximate an asymptotic value — the parameter usually referred to as the *convergence depth* —, different catalogs yield differing conclusions. While at least 50% of $V_{pec,LG}(\infty)$ seems to arise within 5000 km s^{-1} or so, the relative importance of distant regions, i.e. at $cz > 10^4 \text{ km s}^{-1}$, is still an unsettled matter. Scaramella *et al.* (1989) first suggested that the Shapley Supercluster at $cz \sim 13,000 \text{ km s}^{-1}$ could play an important role in affecting the LG motion. The more recent result of Lauer and Postman (1994), confirmed by the reanalysis of Colless (1995), has brought added attention to the possibility that much power in the peculiar velocity field may arise from scales in excess of $cz = 10000 \text{ km s}^{-1}$.

6.2 Clusters to $cz \simeq 9000 \text{ km s}^{-1}$

Using the template described in section 3, [11] have obtained the V_{pec} of 24 clusters and groups out to $cz \simeq 9000 \text{ km s}^{-1}$. As discussed in section 5, their values of V_{pec} are typically smaller than $\sim 500 \text{ km s}^{-1}$, in disagreement with previous measurements of cluster velocities (cf. fig. 2). The larger values of

V_{pec} are observed for relatively nearby groups and for objects in the “Great Attractor” region. The V_{pec} field of the clusters with $4000 < cz < 9000$ km s⁻¹ appears fairly quiescent. Furthermore, the dipole motion of the cluster V_{pec} field, in the Local Group (LG) reference frame, clearly exhibits the “reflex motion” of the LG, i.e. both the dipole apex direction and amplitude of the cluster V_{pec} field mimics that of the CMB dipole:

$$\begin{aligned} V_{clu} &= 577 \pm 101 \quad \text{vs.} \quad V_{cmb} = 627 \pm 22 \\ l_{clu} &= 272 \pm 20 \quad \text{vs.} \quad l_{cmb} = 276 \pm 2 \\ b_{clu} &= +31 \pm 17 \quad \text{vs.} \quad b_{cmb} = +30 \pm 2, \end{aligned}$$

a good agreement, given that only 14 clusters are used for the dipole calculation. Cluster V_{pec} ’s have typical errors of 2–5% of their systemic velocity.

6.3 Field Galaxies to $cz \simeq 6500$ km s⁻¹

In a collaboration referred to as “SCI”, M. Haynes, J. Salzer, G. Wegner, L. da Costa, W. Freudling and this author have obtained V_{pec} for a sample of ~ 1600 field spirals, using the TF relation with I band CCD photometry. Their data, which extends to $\text{Dec} = -30^\circ$, has been combined with the southern data of Mathewson *et al.* (1992), and trimmed to conform with uniform completeness criteria, to produce an all-sky data set which evenly samples a volume of 6,500 km s⁻¹ radius. The data of [18] have been reprocessed for consistency with the northern data, yielding a homogeneous set of V_{pec} measurements.

Similarly to what is observed for clusters, the V_{pec} of field objects measured in the LG reference frame clearly reflects the motion of the LG with respect to the CMB, suggesting that the LG motion with respect to the CMB is largely a local phenomenon, not involving the majority of the volume subtended by the sample. Table 1 exhibits the dipole amplitudes and apices of the field spirals, segregated by redshift shells, and compared to the analogous quantities for the CMB dipole. It is clear that the outer shells of the sampled volume approach rest with respect to the CMB, and that the coherence length of the LG motion does not appear to significantly exceed the radius of the sampled volume. Note, however, the remarks in Strauss (this volume).

6.4 A Test of the Lauer–Postman Bulk Flow

The cluster and field samples described in the two preceding sections have been combined to test the Lauer and Postman (1994; LP) bulk flow. The

V_{cmb} Window	$V_{pec}(LG)$	l	b	Nr.
All	417 ± 28	253 ± 09	37 ± 03	1585
2000 – 3000 km s ⁻¹	333 ± 41	268 ± 16	41 ± 08	235
3000 – 4000 km s ⁻¹	437 ± 57	242 ± 20	24 ± 05	303
4000 – 5000 km s ⁻¹	551 ± 62	236 ± 24	37 ± 05	372
5000 – 6000 km s ⁻¹	566 ± 81	281 ± 15	24 ± 15	270
CMB	627 ± 22	276 ± 03	30 ± 03	

Table 1: Dipoles of the Peculiar Velocity Field

latter measured the dipole of the distribution of brightest elliptical galaxies in 119 clusters distributed over a volume of $\sim 15,000$ km s⁻¹radius. They found that the reference frame defined by the group of clusters is in motion with respect to the CMB at 689 ± 178 km s⁻¹, towards galactic coordinates $(343^\circ, +52^\circ)(\pm 23^\circ)$. This direction is roughly orthogonal to the CMB apex.

Giovanelli *et al.* (1996b) have selected galaxies and clusters with measured V_{pec} in their cluster and field samples, contained within two cones of 30° aperture, directed respectively toward the apex and the antapex of the LP bulk flow. Figure 3 displays V_{pec} , measured in the CMB reference frame, for galaxies and clusters within the two cones. In both cones, the measured V_{pec} fail to match the large amplitude of the LP flow. In Figure 4, the data displayed in fig. 3 are binned by shells of radial velocity, and apex and antapex cones are added in opposition, so that the sign is that of the net velocity in the LP apex direction. The median V_{pec} within a redshift of 5000 km s⁻¹ hovers between 0 and 350 km s⁻¹, while beyond that distance the component of the flow in the LP apex direction subsides to values undistinguishable from zero. An average bulk flow with respect to the CMB as large as 689 km s⁻¹ in that direction can be excluded for galaxies within the volume subtended by these data.

6.5 A *Potent* Reconstruction of the Mass Density Field

The SFI data was used by da Costa *et al.* (1996) to obtain a reconstruction, shown in Figure 5, of the three-dimensional V_{pec} and density fields, using the *Potent* algorithm developed by Bertschinger and Dekel (1989); see also

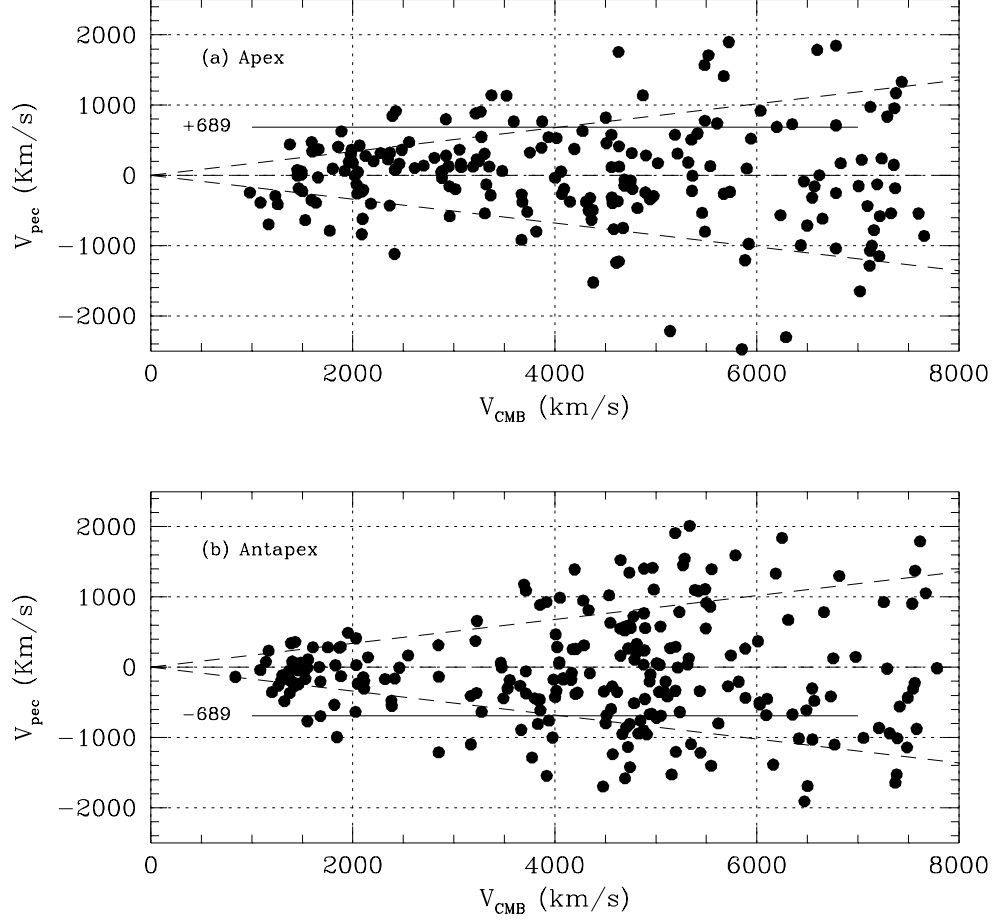


Figure 3: (a) Peculiar velocities of spiral galaxies in the LP apex cone. Both the radial velocity and the peculiar velocity are measured in the CMB reference frame. Dashed lines refer to uncertainties deriving from a mean TF scatter of 0.35 mag. The $+689 \text{ km s}^{-1}$ line refers to the amplitude of the LP bulk flow. (b) Analogous to (a), except that it refers to the antapex cone.

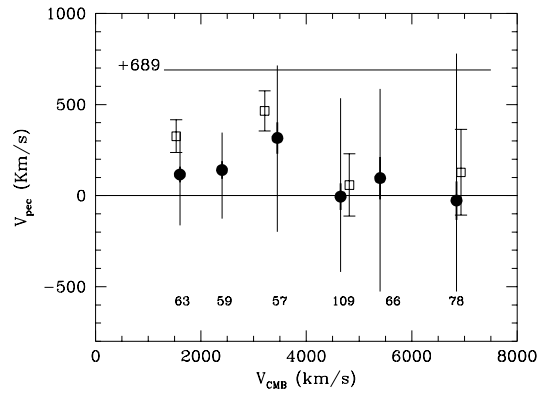


Figure 4: Median V_{pec} of field galaxies (filled symbols) and V_{pec} of four clusters (unfilled symbols) in the apex-antapex cones of the LP bulk flow. Objects in the antapex have been added in apposition to those in the apex cone. Numbers at bottom identify the number of galaxies used in each bin. The $+689 \text{ km s}^{-1}$ horizontal line refers to the LP bulk flow amplitude. Thin error bars outline the range spanned by data within the two inner quartiles, and thick error bars approximate a standard error on the median. The clusters included in the plot are Eridanus, ESO508, A3574 and A400.

[7]. The main characteristics of the reconstruction are similar to those illustrated in recent reconstructions based on Mark III data ([7]), differing in the following details: (i) the outline of the density field in fig. 5 qualitatively resembles that obtained from redshift catalogs, i.e. the mass distribution mimics that of the luminous galaxies better than previous reconstructions; this should help the convergence of techniques aimed at estimating Ω_0 ; (ii) the region between the Local Group and the Perseus and Coma superclusters is dominated by voids; (iii) the Great Attractor appears to be a somewhat closer feature than previously found. While it is important to underscore the similarities between the various density reconstructions obtained from peculiar velocity catalogs, suggesting that real features of the density field are being identified, it is also necessary to keep in mind that the broad window averaging required by reconstruction algorithms yield only the coarsest features, and details at the edges of the reconstructed maps are largely unreliable.

7 The Hubble Constant

Recent HST measurements of Cepheid distances to galaxies in the Virgo and Fornax clusters (see Livio *et al.* 1996) have made possible better estimates of the value of H_0 . One of the thorny issues encountered is the uncertainty on V_{pec} of the clusters in which the galaxies with measured distances are assumed to reside. Expediently, estimates of the distance ratio between the given clusters and Coma are used, so that the uncertainty of the exercise is reduced as the ratio V_{pec}/cz for the given cluster to that of Coma.

The *velocity calibration* of the TF template relation discussed above is significantly more accurate than the ratio V_{pec}/cz of any single cluster. The accuracy of the estimate of H_0 can thus be improved by using the TF relation. In Figure 6, the template relation discussed in section 3 is plotted for different values of $h = H_0/100$ (which is not constrained by the kinematical calibration of the TF relation), and the location of the galaxies with Cepheid distances, which are suitable for TF use. The best match between template and Cepheid distances is for $H_0 = 70 \pm 6 \text{ km s}^{-1}$. Apart from the uncertainty on the Cepheid P-L zero point calibration, the main sources of uncertainty derive from (a) the number N_c of good quality TF calibrators (galaxies with primary distances) and (b) the accuracy of the *velocity calibration* of the TF template relation. As N_c increases thanks to ongoing HST efforts, an improvement of (b) can be achieved by obtaining TF distances of a number

Figure 5: Potent reconstruction of the density and peculiar velocity field using the SFI sample. See text for details.

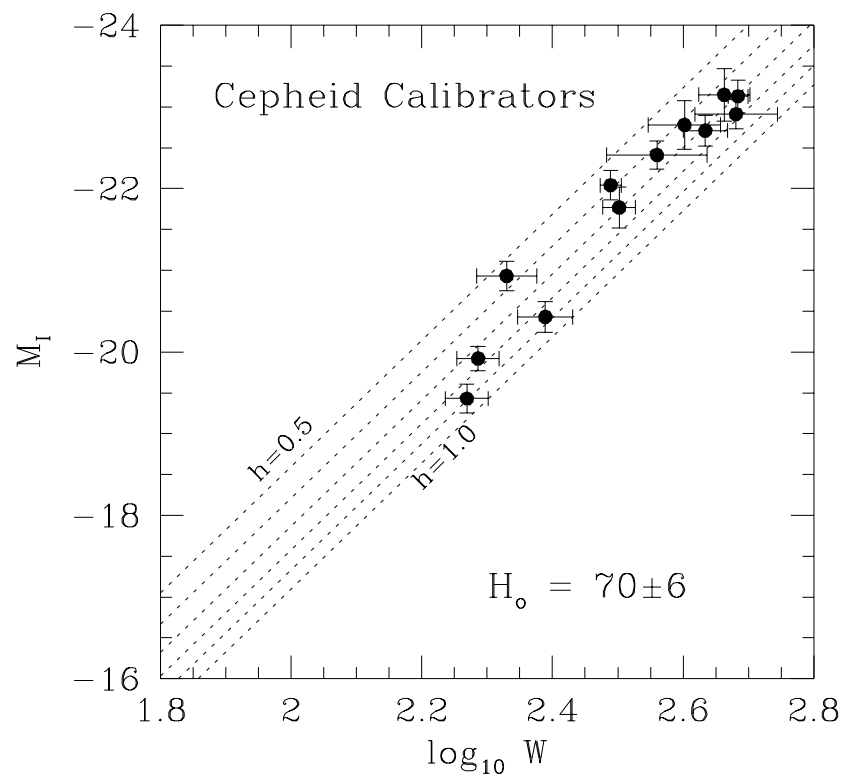


Figure 6: TF Calibrators with available Cepheid distances, superimposed on a grid of TF template relations plotted for different values of h .

of more distant clusters than those currently involved in constructing our template.

8 TF Work in Progress

Here we refer to work in progress other than that reported in the presentation of Strauss (this volume). The main limitations to further applications of the TF technique to the measurement of peculiar velocities are: (a) one of accuracy of the method, which for relatively bright galaxies is restricted to 0.25 to 0.30 mag per single object, and (b) one of accuracy of the parameters — mainly the kinematical zero point — of the TF template relation. On the first part, explorations towards restricting the scatter of the method by inclusion of secondary parameters, such as color, surface brightness, etc., or by using photometry farther in the infrared, have not produced significant improvements. Under current circumstances, excluding low luminosity galaxies from TF analysis appears to be the safest route to obtaining tighter relations. Regarding the quality of the TF template, there is significant room for improvement, which can be achieved by sampling clusters at larger distances than those used to date. An increase of the number, of the regularity of the sky coverage and of the mean distance of the clusters to be used for the definition of the TF template relation can significantly reduce the amplitude of the systematic errors still present in TF analysis. For field objects, dense sampling can produce a valid description of the peculiar velocity field out to $cz \sim 10,000 \text{ km s}^{-1}$. It would thus be desirable that current V_{pec} surveys be extended to that redshift.

We conclude by referring to two such extensions of the TF effort:

- (1) M. Haynes and this author are currently expanding the SCI sample to include approximately 2000 objects with available 21cm spectroscopy, North of -30° . The necessary I band photometry is half-way done, and the project will be concluded in 1997.
- (2) D. Dale, M. Haynes, E. Hardy, L. Campusano, M. Scodeggio and this author are obtaining TF data for 500 galaxies in 80 clusters extending out to $cz \sim 20,000 \text{ km s}^{-1}$. This sample will provide a kinematical reference frame of high accuracy for the calibration of the TF relation, as well as an accurate insight in the issue of bulk flows on very large scales. This project is expected to be concluded in early 1998.

The author wishes to acknowledge the contributions of his collaborators

in several of the results mentioned in this report, namely L. Campusano, P. Chamaraux, L. da Costa, D. Dale, M. Haynes, T. Herter, J. Salzer, M. Scodeggio, N. Vogt, G. Wegner. This work was supported by the National Science Foundation grant AST94–20505.

References

- [1] Aaronson, M. Bothun, G.D., Mould, J.R., Huchra, J., Schommer, R. and Cornell, M. 1986, ApJ 302, 536
- [2] Bahcall, N.A., Gramann, M. and Cen, R. 1994, ApJ 436, 23
- [3] Bahcall, N.A., and Oh, S.P. 1996, ApJ 462, L49
- [4] Bertschinger, E. and Dekel, A. 1989, ApJ (Lett.) 335, L5
- [5] Colless, M. 1995, AJ 109, 1937
- [6] da Costa L.N., Freudling, W., Wegner, G., Giovanelli, R., Haynes, M.P. and Salzer, J.J. 1996, ApJ (Lett.) in press
- [7] Dekel, A. 1994, ARAA 32, 371
- [8] Djorgovski, S. and Davis, M. 1987, ApJ 313, 59
- [9] Dressler, A. et al. 1987, ApJ 313, 42
- [10] Giovanelli, R. 1996, in *The Extragalactic Distance Scale*, M. Livio, M. Donahue, N. Panagia, eds., Cambridge:Cambridge, in press
- [11] Giovanelli, R., Haynes, M.P., Herter, T., Vogt, N.P., da Costa, L.N., Freudling, W., Salzer, J.J. and Wegner, G. 1996a, AJ submitted
- [12] Giovanelli, R., Haynes, M.P., Wegner, G., Salzer, J.J., da Costa, L.N. and Freudling, W. 1996, ApJ (Lett.) 464, L99
- [13] Jørgensen, I., Franx, M. and Kjørgaard, P. 1996, MNRAS 280, 167
- [14] Lauer, T.R. and Postman, M. 1994, ApJ 425, 418
- [15] Livio, M., Donahue, M. and Panagia, N. 1996, eds. of *The Extragalactic Distance Scale*, Cambridge:Cambridge, in press

- [16] Lubin, L.M., Cen, R., Bahcall, N.A. and Ostriker, J.P. 1996, ApJ 460, 10
- [17] Lucey, J.R., Gray, P.M., Carter, D. and Terlevich, R.J. 1991, MNRAS 248, 804
- [18] Mathewson, D.S., Ford, V.L. and Buckhorn, M. 1992, ApJS 81, 413
- [19] Moscardini, L., Branchini, E., Tini–Brunozzi, P., Borgani, S., Plionis, M. and Coles, P. 1996, preprint astro-ph/9511066
- [20] Mould, J.R., Staveley–Smith, L., Schommer, R.A., Bothun, G.D., Hall, P.J., Han, M., Huchra, J.P., Roth, J., Walsh, W. and Wright, A.E. 1991, ApJ 383, 467
- [21] Rhee, M.–H. 1996, Ph.D. Thesis, U. of Groningen
- [22] Rubin, V.R., Ford, W.K., Thonnard, N., Roberts, M.S. and Graham, J.A. 1976, AJ 81, 687
- [23] Scaramella, R. et al. 1989, Nature 338, 562
- [24] Scaramella, R., Vettolani, G. and Zamorani, G. 1994, ApJ 422, 1
- [25] Scodeggio, M., Solanes, J.M., Giovanelli, R. and Haynes, M.P. 1995, ApJ 444, 41
- [26] Scodeggio, M., Giovanelli, R. and Haynes, M.P. 1996, AJ submitted
- [28] Strauss, M.A. and Willick, J.A. 1995, Physics Reports 261, 271
- [28] Tini–Brunozzi, P., Borgani, S., Plionis, M., Moscardini, L. and Coles, P. 1996, MNRAS in press
- [29] Tully, R.B. and Fisher, J.R. 1977, AA 54, 661
- [30] White, S.D., Navarro, J.F., Evrard, A.E. and Frenk, C.S. 1993, *Nature* 366, 429

